AGU ADVANCING EARTH AND SPACE SCIENCES

Geophysical Research Letters

RESEARCH LETTER
10.1029/2025GL119595

Special Collection:
Integrating In Situ, Remote Sensing, And Physically Based Modeling Approaches to Understand Global Freshwater Ice Dynamics

Bayesian Estimates of Ice Optical Properties for Lake Ice Modeling

G. Donini[1], C. Agostinelli[2], G. A. Weyhenmeyer[3], G. Kirillin[4], M. Leppäranta[5], G. E. Zdorovennova[6], I. A. Aslamov[7], J. A. Culpepper[8], H. A. Dugan[9], I. V. Fedorova[10], E. Jakobsson[3], R. L. North[11], Iu.S. Novikova[6], N. I. Palshin[6], N. J. T. Pearce[12], J. Robinson[13], K. Shchapov[14], K. Vikström[3], M. A. Xenopoulos[12], X. Yang[15], R. E. Zdorovennov[6], and S. Piccolroaz[1]

[1]Department of Civil, Environmental and Mechanical Engineering, University of Trento, Trento, Italy, [2]Department of Mathematics, University of Trento, Trento, Italy, [3]Institute of Ecology and Genetics/Limnology, Uppsala University, Uppsala, Sweden, [4]Department of Ecohydrology and Biogeochemistry, Leibniz-Institute of Freshwater Ecology and Inland Fisheries, Berlin, Germany, [5]Institute of Atmospheric and Earth Sciences, University of Helsinki, Helsinki, Finland, [6]Northern water problems Institute, Karelian Research Centre of the Russian Academy of Sciences, Petrozavodsk, Russia, [7]Limnological Institute, Siberian Branch of the Russian Academy of Sciences, Irkutsk, Russia, [8]Department of Biology, York University, Toronto, ON, Canada, [9]Center for Limnology, University of Wisconsin–Madison, Madison, WI, USA, [10]Institute of Botany after A. Takhtajyan National Academy of Sciences of the Republic of Armenia, Yerevan, Armenia, [11]School of Natural Resources, University of Missouri, Columbia, MO, USA, [12]Department of Biology, Trent University, Peterborough, Ontario, Canada, [13]Department of Biological Sciences, Rensselaer Polytechnic Institute, Troy, NY, USA, [14]Cawthron Institute, Nelson, New Zealand, [15]Department of Earth Sciences, Southern Methodist University, Dallas, TX, USA

Key Points:

- Bayesian modeling provides robust estimates of lake-ice optical properties from a large and diverse data set
- Snow and white ice exert the strongest attenuation of under-ice irradiance and show the largest variability across lakes
- Optical parameters provide key inputs for forecasting under-ice light regimes and improving global lake-ice and climate model projections

Supporting Information:

Supporting Information may be found in the online version of this article.

Correspondence to:

S. Piccolroaz and G. Donini,
s.piccolroaz@unitn.it;
gaia.donini@unitn.it

Citation:

Donini, G., Agostinelli, C., Weyhenmeyer, G. A., Kirillin, G., Leppäranta, M., Zdorovennova, G. E., et al. (2026). Bayesian estimates of ice optical properties for Lake ice modeling. *Geophysical Research Letters*, *53*, e2025GL119595. https://doi.org/10.1029/2025GL119595

Received 24 SEP 2025
Accepted 30 MAR 2026

Author Contributions:

Conceptualization: G. A. Weyhenmeyer, G. Kirillin, M. Leppäranta, H. A. Dugan, M. A. Xenopoulos, X. Yang, S. Piccolroaz
Data curation: G. Donini, G. A. Weyhenmeyer, G. E. Zdorovennova, H. A. Dugan, E. Jakobsson, R. L. North, Iu. S. Novikova, N. I. Palshin, N. J. T. Pearce, J. Robinson, K. Shchapov, K. Vikström, M. A. Xenopoulos, R. E. Zdorovennov

Abstract Ice and snow cover on frozen lakes is a natural barrier to solar radiation, reducing the transfer of energy that controls under-ice thermal dynamics and biological productivity. Direct measurements of under-ice irradiance remain scarce due to logistical constraints. We assembled data from 46 freshwater lakes across the Northern Hemisphere, including 722 daily irradiance observations and ice and snow thickness records. Ice quality data (black ice, white ice, and snow cover) were available for 15 lakes (626 measurements). Using this data set and a Bayesian implementation of the Beer-Lambert law, we estimated statistical distributions of albedo and attenuation coefficients. Median albedo values were 0.55 for black ice, 0.60 for white ice, 0.56 for total ice, and 0.94 for snow, with corresponding attenuation coefficients of 0.79, 4.35, 1.75, and 8.96 m^{-1}, respectively. These refined optical properties address critical data gaps, improving under-ice irradiance predictions and enhancing understanding of lake processes under climate-driven ice conditions.

Plain Language Summary The amount of sunlight that passes through lake ice and snow cover in winter plays a major role in regulating under-ice thermal conditions and aquatic biological processes. However, winter conditions make data collection difficult, and measurements of under-ice irradiance (light energy) remain scarce. This lack of data limits our ability to predict biological activity and water movement beneath the ice. In this study, we collected irradiance measurements above and below the ice from 46 freshwater lakes across the Northern Hemisphere with varying ice and snow thickness. For 15 lakes, we also recorded ice quality (black ice and white ice), gathering over 600 daily irradiance records. Using a statistical model, we estimated how different types of ice and snow cover reflect light (albedo) and reduce its penetration into lakes (attenuation coefficients). Our large and diverse data set enabled accurate estimates of light attenuation, with explicit quantification of uncertainty, increasing our understanding of how light penetration differs among frozen lakes of different shapes, sizes, and water quality across the Northern Hemisphere (~41°–62°N). Our findings support improved projections of climate change impacts on lake systems worldwide, with relevance for the research community and for those involved in lake impact assessment and management.

1. Introduction

Lake ice acts as a natural barrier limiting the exchange of matter and energy between the water and the atmosphere (Hampton et al., 2024; Kirillin et al., 2012; Leppäranta, 2023). The limited solar radiation that penetrates through snow and ice represents one of the few, and often the dominant, energy sources in the winter heat budget, driving physical, chemical, and biological processes in lakes (Dugan et al., 2025; Song et al., 2019). Beneath lake ice,

Formal analysis: G. Donini, C. Agostinelli, S. Piccolroaz
Investigation: G. Donini, C. Agostinelli, S. Piccolroaz
Methodology: G. Donini, C. Agostinelli, S. Piccolroaz
Project administration: S. Piccolroaz
Software: G. Donini, C. Agostinelli
Supervision: S. Piccolroaz
Visualization: G. Donini, C. Agostinelli
Writing – original draft: G. Donini, S. Piccolroaz
Writing – review & editing: G. Donini, C. Agostinelli, G. A. Weyhenmeyer, G. Kirillin, M. Leppäranta, G. E. Zdorovennova, I. A. Aslamov, J. A. Culpepper, H. A. Dugan, I. V. Fedorova, E. Jakobsson, R. L. North, Iu.S. Novikova, N. I. Palshin, N. J. T. Pearce, J. Robinson, K. Shchapov, K. Vikström, M. A. Xenopoulos, X. Yang, R. E. Zdorovennov, S. Piccolroaz

water is inversely stratified, and radiative heating of the upper water column drives gravitational instability (Bouffard & Wüest, 2019; Kirillin et al., 2021) which redistributes dissolved gases, nutrients, and non-motile primary producers (e.g., phytoplankton) into the upper water column (Bouffard et al., 2019; Palshin et al., 2019; Pernica et al., 2017). Solar radiation, including the photosynthetically active fraction (PAR, radiation in the 400–700 nm range), that penetrates snow and ice is at a maximum at the water-ice interface. The convective redistribution of resources and organisms into these higher-light conditions supports the growth of primary producers, oxygen production under the ice (Suarez et al., 2019; Vehmaa & Salonen, 2009), and increased feeding opportunities for consumers in an environment with greater visibility (Langbehn & Varpe, 2017). Hence, the penetration of solar radiation through snow and ice plays a central role in the ecological functioning of ice-covered lakes (Bramburger et al., 2023; Garcia et al., 2019; Hampton et al., 2015; Obertegger et al., 2017; Socha et al., 2023; Yang et al., 2020). Accurately quantifying the attenuation of solar radiation is therefore critical for understanding the interplay between winter hydrodynamics and biological activity.

The attenuation of solar radiation in snow and ice is controlled by both thickness and structural composition. Lake ice first forms through congelation as surface water temperatures drop below freezing (0°C) and thickens from below developing into highly transparent "black" ice which appears dark due to weak backscatter from the underlying water (Leppäranta, 2023; Michel & Ramseier, 1971). Later, ice thickens from above when wet snow forms slush that refreezes into a new layer of superimposed ice, known as snow ice or "white" ice because of high backscattering from air pockets. Alongside these two layers, snow can accumulate on top of the ice surface, and slush can form in the snow layer or be contained within the white ice layer (Ashton, 2011; Cheng et al., 2020; Leppäranta, 2023). The composition of snow and ice profiles can therefore vary substantially among lakes and between years due to weather and climate differences.

Two optical properties describe the penetration of solar radiation through snow and ice: albedo (the fraction of reflected radiation relative to the incoming radiation), and the attenuation coefficient (the amount of radiation absorbed or scattered per unit depth) (Petrov et al., 2005). Both properties are influenced by the structural composition of ice and snow, impurities, bubbles, brine content (Arst et al., 2006; Mullen & Warren, 1988), and environmental factors like solar altitude (Jakkila et al., 2009; Lang et al., 2018). These apparent optical properties also change over time as ice thickens, snowpack evolves, and meltwater pools form on the ice surface in spring (Bolsenga, 1981; Fritsen & Priscu, 1999; Leppäranta et al., 2010; Zdorovennova et al., 2013, 2018). Despite inherent temporal variability, the apparent optical properties remain largely stable over the winter season and primarily reflect the dominant structural composition of the snow and ice profile (Bolsenga, 1977; Lang et al., 2018; Mobley, 2001; Mullen & Warren, 1988). Each layer of the snow and ice profile has distinct optical properties. Solar radiation attenuation within ice is mainly caused by gas bubbles (Jakkila et al., 2009; Lei et al., 2011; Mullen & Warren, 1988), which are more abundant in white ice, leading to higher attenuation compared to black ice. Snow strongly attenuates the solar radiation due to air pockets (Kirillin et al., 2012): as little as 13.5 cm of snow can attenuate enough light to inhibit phytoplankton growth (Pernica et al., 2017). Although snow and ice rapidly attenuate solar radiation (Arst et al., 2006; Kirillin et al., 2012), some of the radiation is also backscattered toward the surface and laterally from the underlying layers. This albedo effect persists in snow thinner than ∼10 cm (Perovich, 2007; Zhao et al., 2024) and ice thinner than ∼30 cm (Kirillin et al., 2012).

A reliable estimate of albedo (α) and the diffuse attenuation coefficient of irradiance (k) for different snow and lake-ice compositions is essential to determine under-ice irradiance when direct measurements are unavailable. However, estimating these properties is challenging due to limited observational data from ice-covered lakes (Hampton et al., 2017) largely due to logistical difficulties of accessing monitoring sites (Block et al., 2019). In addition, monitoring is often manual (Bolsenga, 1981) and rarely automated (Aslamov et al., 2021; Lei et al., 2011; Leppäranta et al., 2010; Niu et al., 2025), resulting in sparse measurements across a limited number of lakes and time periods that cannot capture the full range of conditions, especially in terms of the structural composition of snow and ice. A wide range of site- and condition-specific values for α and k are reported in the literature (Figures 1a and 1b) and discussed in the next section. High variation in these measurements is further compounded by measurement errors, especially in ice stratigraphy and snow thickness, with the latter often being uncertain due to wind-drift. Generalizing these values to unmonitored lakes is therefore difficult and can lead to significant uncertainty in under-ice irradiance estimates, motivating the need for a more unified and statistically grounded approach.

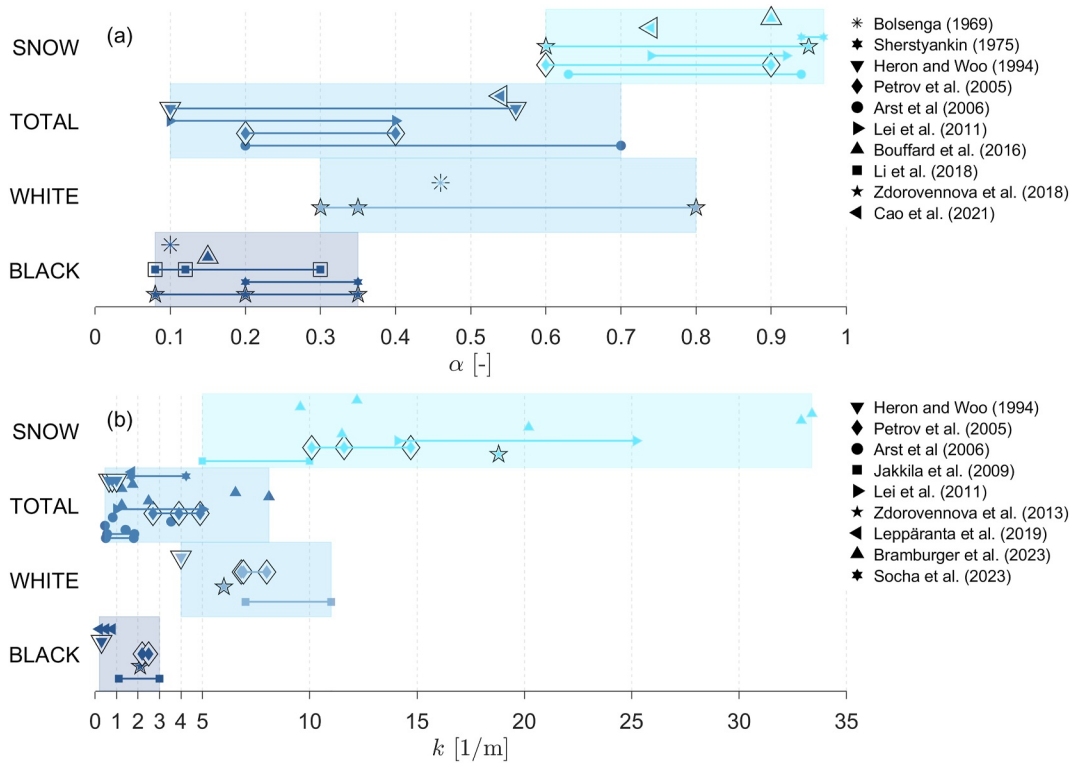

Figure 1. Literature values of (a) albedo (α) and (b) diffuse attenuation coefficient (k) for black ice, white ice, total ice, and snow. Different markers indicate individual studies. Bordered markers indicate total shortwave irradiance, unbordered markers indicate PAR measurements. Connected markers indicate a range of reported values, and a third marker, when present, represents the mean.

In this study, we address current uncertainties in estimating lake-ice optical properties by developing a framework to overcome fragmented descriptions of these properties. First, we assembled a comprehensive data set of ice and snow thickness measurements together with corresponding irradiance data from multiple lakes across the Northern Hemisphere, including previously unpublished observations. We then applied a Bayesian model to infer optical properties while accounting for natural variability across different lake and ice-snow conditions. This approach yields probabilistic estimates of α and k for black ice, white ice, total ice (i.e., combined black and white ice), and snow.

2. Material and Methods

2.1. Variability of α and k in the Literature

We compiled previously published values of α and k for lake ice and snow to highlight their variability across different studies and to provide reference values for subsequent modeling. The available literature values are predominantly from lakes in the Northern Hemisphere, particularly Russia (Bouffard et al., 2019; Petrov et al., 2005; Sherstyankin, 1975; Zdorovennova et al., 2018), Finland (Arst et al., 2006; Jakkila et al., 2009; Lei et al., 2011; Leppäranta et al., 2019), Estonia (Arst et al., 2006; Lei et al., 2011), China (Cao et al., 2021; Li et al., 2018), the United States (Bolsenga, 1969; Bramburger et al., 2023; Socha et al., 2023), and Canada (Heron & Woo, 1994) (Figure 1). Optical properties in these studies were derived from field measurements of either PAR or total shortwave irradiance (0.3–3.0 μm). Beyond the expected differences in α and k among snow and ice types (Figure 1), substantial variability across studies exists, especially in α, and in k for snow. The observed variability in optical properties highlights the need for a unified modeling approach. Summary statistics derived from the literature data are reported in Table 1, and the corresponding mean values of k and α were used to guide our modeling.

Table 1
Comparison of Mean, Median, and Standard Deviation Between Literature Values (Figure 1) and the Fixed Components of the Bayesian Model, With Ranges and 90% Confidence Bounds Reported for Literature and Model, Respectively

	Literature					Model			
	n	Mean	Median	std	Min-max	mean	median	std	90% c.b.
α_b (–)	5	0.17	0.15	0.07	0.08–0.35	0.52	0.55	0.18	0.45–0.76
α_w (–)	2	0.41	0.41	/	0.3–0.8	0.60	0.60	0.10	0.45–0.78
α_t^* (–)	5	0.37	0.33	0.12	0.1–0.7	0.60	0.59	0.16	0.35–0.90
α_t^{**} (–)						0.55	0.56	0.08	0.42–0.68
α_s (–)	7	0.82	0.79	0.08	0.6–0.97	0.94	0.94	0.02	0.91–0.96
α_s^* (–)						0.93	0.93	0.02	0.90–0.95
α_s^{**} (–)						0.90	0.90	0.03	0.84–0.94
k_b (m^{-1})	5	1.24	1.1	0.88	0.2–3	0.81	0.79	0.40	0.24–1.46
k_w (m^{-1})	4	6.48	6.45	2.07	4–11	4.66	4.35	1.55	2.94–7.35
k_t^* (m^{-1})	17	2.49	1.7	2.09	0.46–8.1	2.19	2.15	0.53	1.42–3.06
k_t^{**} (m^{-1})						1.75	1.75	0.36	1.17–2.35
k_s (m^{-1})	10	17.73	15.5	9.22	5–33.4	8.96	8.96	0.97	7.35–10.54
k_s^* (m^{-1})						8.89	8.89	0.92	7.37–10.37
k_s^{**} (m^{-1})						8.23	8.28	1.07	6.38–9.89
c (m)	4	0.019	0.020	0.009	0.007–0.03	0.020	0.019	0.003	0.016–0.024
c^* (m)						0.019	0.019	0.002	0.015–0.023
c^{**} (m)						0.019	0.019	0.003	0.015–0.024

Note. The column n indicates the number of literature values used. A single asterisk (*) denotes variables from the model based on the same subset of lakes used for the ice quality model but built using total ice, while a double asterisk (**) refers to the model built using total ice and the entire data set.

2.2. Data Set Assembly

We assembled a data set of optical and cryospheric measurements from 46 lakes across the Northern Hemisphere, combining original observations from independent field campaigns conducted by the authors with data compiled from previously published studies. The data set includes ice and snow thickness, ice type, irradiance above the ice (E_{ai}), and irradiance reaching the water immediately beneath ice cover (E_{ui}). Lake locations are shown in Figure 2a and lake-specific details, including references to previously published data sets (Table S1 in Supporting Information S1), are available in the Supporting Information S1.

In the data set, thickness refers to snow thickness and total ice thickness. When ice quality data were available, total ice was divided into black and white ice. Irradiance measurements varied in frequency across lakes and were taken using both cosine and spherical sensors (see Table S1 in Supporting Information S1). Spherical sensors were used only in the Canadian lakes Blackstrap, Broderick, and Diefenbaker. Total shortwave irradiance was measured in Lake Vendyurskoe and Lake Onega (Russia) as energy flux (W m^{-2}), while in all other lakes irradiance was recorded in the PAR range as photon flux (μmol m^{-2} s^{-1} or equivalent photon-based units). Here, attenuation coefficients are interpreted as effective parameters consistent with the spectral range and sensor type used in each lake. Under the predominantly diffuse light conditions beneath snow and ice, and because attenuation estimates rely on the relative vertical change of irradiance, instrument-related differences are expected to be small relative to the variability associated with ice-snow properties (Arst et al., 2006), and similarly, band-related differences are expected to remain secondary to structural variability within snow and ice layers.

To ensure consistency, we only included daily observations in the data set where all three components (E_{ai}, E_{ui}, and ice-snow cover thickness) were available. No data reconstruction was performed. When continuous irradiance measurements were available throughout the day, the observation closest to noon was selected to minimize diurnal variability. When only daily measurements were available and the time of measurement was not recorded, the reported daily value was retained, as it represents daytime conditions. Under-ice PAR measurements below

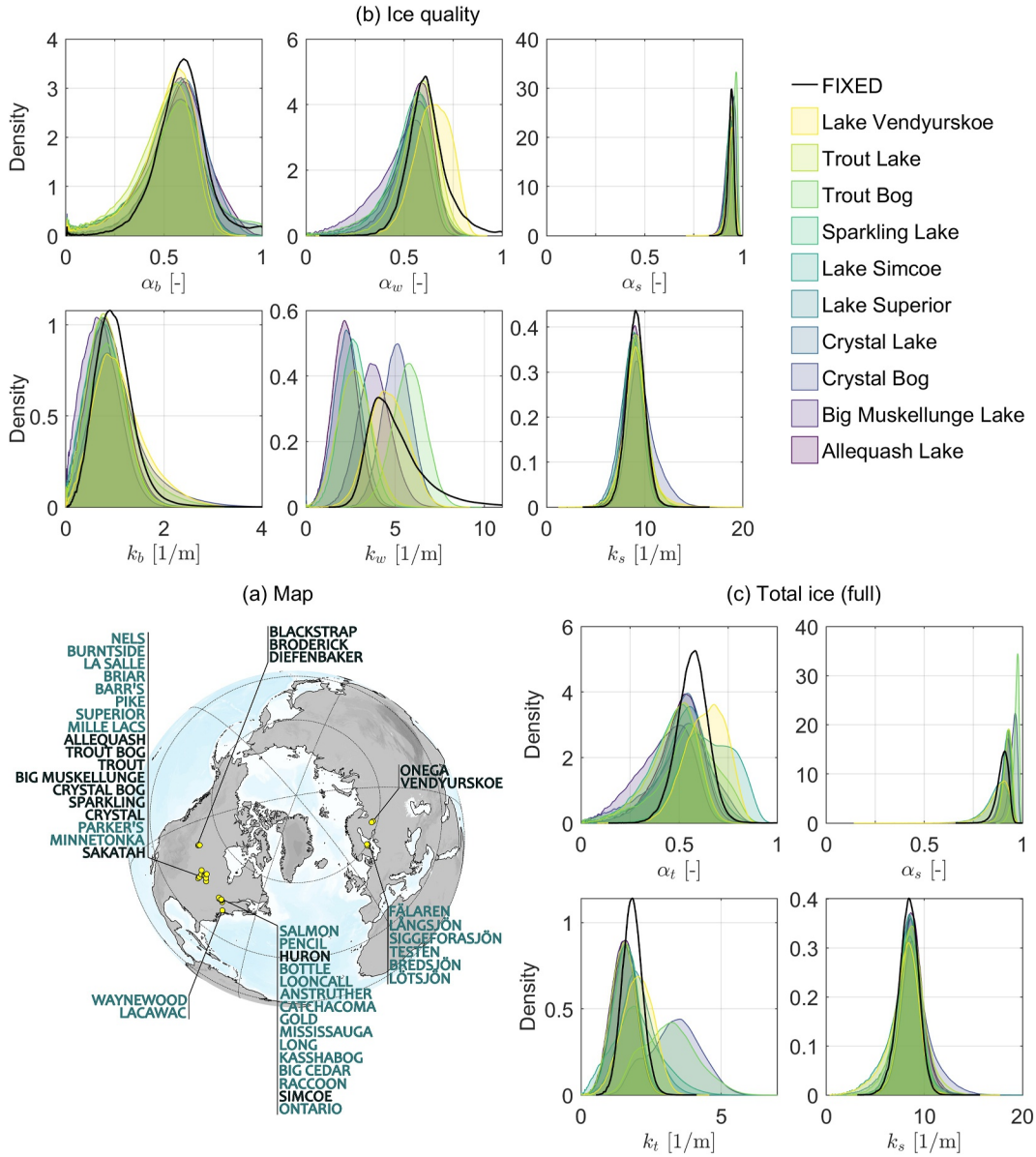

Figure 2. Locations of lakes included in the data set are shown in (a). Lake names in black indicate lakes with ice quality data, while names in gray correspond to lakes with only total ice thickness measurements. Panels (b, c) show posterior probability distributions of albedo (α) and diffuse attenuation coefficients (k) obtained from ice quality data (b) and from total ice using the full data set (c). The black line shows the pdf of the fixed component of the mixed model, while colored lines represent pdfs incorporating both the fixed and lake-specific random components for lakes with more than 10 measurements.

0.125 μmol m^{-2} s^{-1} were excluded to ensure robust low-light measurements and to avoid uncertainties near instrument detection thresholds.

The final data set includes 722 measurements from 46 lakes. For 31 lakes, only total ice thickness was available (54 measurements). Ice quality data were recorded for 15 lakes (626 measurements), although in 3 of these lakes only total ice thickness was reported for certain periods (42 measurements).

2.3. Bayesian Inference of Optical Parameters

We adopted the Beer-Lambert absorption law as a first-order, physically based description of irradiance attenuation within the snow–ice cover, assuming exponential decay and stepwise-varying attenuation coefficients (k (m^{-1}) for black ice, white ice, and snow, denoted by the subscripts b, w, and s, respectively:

$$E_{ui} = (1-\alpha)E_{ai}e^{(-k_b h_b - k_w h_w - k_s h_s)}, \tag{1}$$

where E_{ui} is the under-ice irradiance, E_{ai} is the irradiance above the ice-snow cover, and α (–) is the albedo of the ice-snow cover, and h [m], with the corresponding subscript, denotes the thickness of each layer. Both E_{ui} and E_{ai} can be expressed in W m^{-2} or μmol $m^{-2}s^{-1}$, but the units must be consistent between them.

Layer thicknesses and irradiance measurements (E_{ui} and E_{ai}) were obtained from the data set, while k and α, were parameters to be estimated. When no data on ice structure were available, we applied an alternative approach replacing black and white ice thicknesses and attenuation coefficients in Equation 1 by those of total ice, denoted as h_t and k_t, treating the ice cover as a single optical layer. While simplifying the model and reducing the accuracy, the approach is practical for cases when only the total ice thickness is reported.

We implemented a correction for snow albedo to account for the albedo of the underlying ice layer, which becomes non-negligible for thin snow covers. Based on experimental studies (Perovich, 2007) and field measurements (Grenfell & Perovich, 2004; Zhao et al., 2024), snow albedo follows an exponential decay, described by the formula:

$$\alpha_{s,corr} = \alpha_s - (\alpha_s - \alpha_{ul})\, e^{(-h_s/c)}, \tag{2}$$

where α_s is the asymptotic snow albedo, α_{ul} is the albedo of the underlying ice (black or white), h_s is the snow thickness, and c is a decay constant, typically $\sim 10^{-2}$ m (Grenfell & Perovich, 2004; Zhao et al., 2024), making this correction relevant for snow layers $\lesssim$10 cm (309 measurements in the data set). In the model, the coefficient c was calibrated and, as a snow property, assumed identical for underlying black or white ice. The same correction was also applied when only total ice was considered.

To explicitly quantify uncertainty, we used a Bayesian framework to infer probability distributions of α, k, and c by implementing the linearized form of Equation 1:

$$-\ln(E_{ui}/E_{ai}) = -\ln(1-\alpha) + k_b h_b + k_w h_w + k_s h_s, \tag{3}$$

where α denotes the albedo of the uppermost layer, selected through an indicator function of the surface type, and incorporates the correction of Equation 2 when applicable. This approach was also applied to the total ice thickness data. The linearization is advantageous because it converts multiplicative relationships into an additive form, thereby improving the stability of the inference process. Additionally, taking the logarithm of E_{ui}/E_{ai}, which spans several orders of magnitude, reduces the impact of heteroscedasticity in the data.

We define θ as the vector of parameters to be estimated. When ice quality information is available, $\theta = (\alpha_s, \alpha_w, \alpha_b, k_s, k_w, k_b, c)$; when only total ice thickness is known, $\theta = (\alpha_s, \alpha_t, k_s, k_t, c)$. According to Bayes' theorem:

$$P(\theta|y) \propto P(\theta)P(y|\theta), \tag{4}$$

where $P(\theta|y)$ is the posterior distribution of the parameters given the observations $y = -\ln(E_{ui}/E_{ai})$, $P(\theta)$ is the prior distribution representing initial knowledge or assumptions about the parameters, and $P(y|\theta)$ is the likelihood, which expresses the probability of observing the data given the parameters θ and reflects how well the model fits the observations. The prior distributions of the physical parameters in θ were centered on literature mean values (Table 1), and standard deviations were set to five times the mean, producing broad, effectively non-informative priors that minimize constraints on the inference. The likelihood was modeled by assuming each observation y is drawn from a normal distribution: $y \sim \mathcal{N}(\mu(h_b, h_w, h_s, \theta), \phi)$, where $\mu(h_b, h_w, h_s, \theta)$ is the mean model prediction computed from the right-hand side of Equation 3, and ϕ is the variance.

Because the data set spans diverse lake locations, trophic states, weather conditions, and instruments, we applied a mixed-effects Bayesian model (Jiang & Nguyen, 2021; Wu, 2009) to evaluate how this heterogeneity influences the estimation of optical parameters. In this framework, lake-specific random effects were added to the global (fixed) parameter estimates, the latter being assumed to be constant across all observations. This approach enabled the detection of potential lake-specific patterns, while also accounting for unbalanced sampling, mitigating the influence of lakes with more measurements. Random effects were included for all physical parameters except c, which was assumed to be lake-independent.

The model was implemented in Stan (Stan Development Team, 2024), where the posterior distribution of the parameters was sampled using the NUTS-HMC (No-U-Turn Sampler Hamiltonian Monte Carlo) algorithm (Hoffman & Gelman, 2014), an efficient method for exploring complex, high-dimensional parameter spaces. Further details on the model are provided in Text S1 in Supporting Information S1.

To evaluate model performance, the Continuous Ranked Probability Score (CRPS) (Gneiting & Raftery, 2007) was calculated for each observation as:

$$CRPS(F,x) = \int_{-\infty}^{+\infty} (F(y) - H(y-x))^2 dy, \tag{5}$$

where $F(y)$ is the cumulative distribution function of the model prediction for $y = -\ln(E_{ui}/E_{ai})$, x is the observed value, and $H(y-x)$ is the Heaviside step function, equal to 1 for $y \geq x$ and 0 otherwise. CRPS integrates the squared difference between the cumulative distribution functions $F(y)$ and $H(y-x)$, capturing both the accuracy of the predicted median and the overall shape of the predictive distribution. Lower CRPS values indicate better probabilistic predictions, as they reflect smaller deviations between the predicted distribution and the observed value. This metric was adopted because the model produces predictive probability distributions rather than single-point estimates, making deterministic metrics less appropriate.

3. Results and Discussion

Median parameter estimates from the Bayesian model were $\alpha_b = 0.55$, $\alpha_w = 0.60$ and $\alpha_s = 0.94$ for albedoes, and $k_b = 0.79$, $k_w = 4.35$ and $k_s = 8.96$ m^{-1} for diffuse attenuation coefficients when ice quality data were considered. Using the full data set with total ice, estimates were $\alpha_t = 0.56$, $\alpha_s = 0.90$, $k_t = 1.75$ and $k_s = 8.28$ m^{-1}. Similar results were obtained when using the subset of lakes from the ice-quality model but treating ice as a single layer. Posterior probability distributions (pdfs) of the α and k coefficients are shown in Figures 2b and 2c, and summary statistics are reported in Table 1 alongside the ranges observed in the literature (Figure 1).

Overall, the optical properties estimated in this study align with values from the literature, apart from some notable differences in k_s and α_b (see Table 1). The estimated k_s is approximately half the literature median, but remains within the range of published data. k_s is influenced by snow metamorphism, structure, liquid water content, and density which can change substantially over the winter season (Warren, 1982). Isolated measurements may not be generalizable to the entire period of snow and ice cover, offering an explanation for the high variability and differences in k_s observed. The estimated α_b is higher than literature values. This estimate is based on only 15 single-layer observations of black ice collected in spring (March–April), when lower albedo is actually expected as wet ice approaches the albedo of open water. However, because α_b is jointly inferred with k_b and enters the albedo correction when snow overlies black ice together with α_s and c (all of which are informed by a much larger data set), the resulting estimate should be interpreted as an effective season-averaged value. The posterior pdfs show distinct peaks and limited spread (Figures 2b and 2c) indicating that parameter estimates were well-constrained by the data and reliable. α_s was the most well-constrained parameter, showing narrow and consistent distributions across lakes, particularly when ice quality information was available. We note that α_s here represents the asymptotic value, with the effective snow albedo evaluated using the decay constant c in Equation 2. The parameter c itself showed very small variance and a median value highly consistent with literature values in both the ice quality and total ice cases (see Table 1 and Figure S1 in Supporting Information S1). Among-lake variability in optical properties was minimal, except for k_w which exhibited considerable variability as described through the random effects component of the model. Relative to the pdf of the fixed component (black curve), which excludes random effects, lakes were split into three distinct groups. The pdf

peaks of the two bog lakes (Trout Bog and Crystal Bog, Wisconsin, USA) had the highest k_w values; Lake Vendyurskoe (Russia) was close to the fixed pdf; and all other lakes had lower values. This among-lake variability of k_w, also reflected in k_t, is likely a result of heterogeneity in white ice (e.g., mixed ice and slush layers) and the influence of lake water quality. For example, in humic lakes like Trout Bog and Crystal Bog, white ice often contains lake water rich in colored dissolved organic matter (cDOM) that becomes trapped during ice crystallization, resulting in higher diffuse attenuation coefficients. In contrast, black ice forms with fewer impurities (i.e., trapped gas bubbles) and is more homogeneous than white ice. Consistent with the literature (Figure 1b), we observed that the posterior distributions of k_w were much broader than those of k_b suggesting that white ice heterogeneity exerts a stronger influence on lake-ice optical properties than black ice. Likewise, k_s distributions were broader than k_b. Although k_s was highest and spanned a large range, the absence of random effects suggests that variation in white ice structure plays a larger role in attenuation than the snow metamorphism discussed above.

The observed values of $\ln(E_{ui}/E_{ai})$ were well-aligned with the medians of the estimated distributions across the full range of variability (Figure 3 and Figures S5–S19 in Supporting Information S1 for individual lakes). The best agreement was achieved with the mixed model based on ice quality data (Figure 3a); the fit of the mixed model with total ice data showed weaker agreement (Figures 3c and 3e). Performance declined in the lower tail when relying solely on the fixed component, particularly for total ice (Figures 3d and 3f), whereas agreement remained stronger for the ice quality case (Figure 3b). Notably, the lower tail is largely contributed by Trout Bog and Crystal Bog (Figure S2 in Supporting Information S1), where total ice contains a higher proportion of white ice (>50%) than other lakes (average 23%; Figure S3 in Supporting Information S1). As previously noted, these lakes exhibit k_w and k_t values that deviate from the fixed component, likely because their highly dystrophic conditions result in ice with higher concentrations of cDOM. The larger proportion of white ice further contributes to poorer estimates, particularly when ice quality is unknown and only the fixed component is used (Figures 3d and 3f).

Model diagnostic plots are corroborated by the CRPS distributions (side panels in Figure 3 and Figure S4 in Supporting Information S1): median CRPS remains below 1 (taken here as a reasonable threshold) for most observations, indicating robust predictive performance, particularly for the mixed models. When using only the fixed component, mean CRPS slightly exceeds 1 in the lower tail ($\ln(E_{ui}/E_{ai}) < -7$ for ice quality, < -6 for total ice). Overall, the fixed component captures irradiance attenuation effectively across lakes with ice quality data. When only total ice is available, results remain reasonable, except in cases of high irradiance attenuation, reflecting the greater thickness and variability of the white ice layer.

Our results confirm that snow and white ice layers exert the strongest attenuation of under-ice irradiance, with snow metamorphism and white ice heterogeneity (k_s, k_w) contributing most to the variability and uncertainty in irradiance estimates. In contrast, black ice properties (k_b) are comparatively stable across lakes and less effective at attenuating incoming irradiance. Because snow and white ice are both strong attenuators and among the most variable components, even small changes in snowfall or melt-refreeze cycles can substantially affect irradiance penetration, with cascading effects on under-ice physical, chemical, and biological processes (Barrett & Wrona, 2025; Kirillin et al., 2012). Likewise, corresponding changes in ice cover duration may further alter the frequency and persistence of snow and white ice layers, either offsetting or exacerbating their impact. These considerations are particularly relevant in the context of ongoing and projected changes in ice and snow regimes. Long-term observations indicate a general thinning of black ice alongside an increasing white-to-black ice ratio, consistent with more frequent snowfall and thaw–refreeze events, though regional responses vary (Culpepper et al., 2024). Climate projections suggest a global mean decline in maximum lake-ice thickness of about 0.23± 0.07 m between 2000 and 2100 (Huang et al., 2022) along with shorter ice cover durations, but regional snow depth forecasts remain uncertain due to spatial and temporal heterogeneity in warming, precipitation timing, and phase (McCrystall et al., 2021; Pongracz et al., 2024). Despite these uncertainties, several contrasting scenarios can be anticipated across the Northern Hemisphere. In mid-latitudes, reduced ice thickness combined with lower snow accumulation and increased liquid precipitation may enhance under-ice irradiance, particularly in southern areas where large interannual variability in ice thickness and duration is already observed (Solarski & Retała, 2020). On the Tibetan Plateau, thinning ice coupled with limited changes in precipitation suggest only a slow increase in irradiance (Huang et al., 2022; Quante et al., 2021). In high-latitude regions, projected increases in snowfall and white ice formation are expected to strongly reduce under-ice irradiance. Finally, in northern Fennoscandia and northwestern Canada, warming and partial snow-to-rain shifts may favor white ice formation, also decreasing light penetration (Ariano & Brown, 2019; Quante et al., 2021; Weyhenmeyer et al., 2022). Given

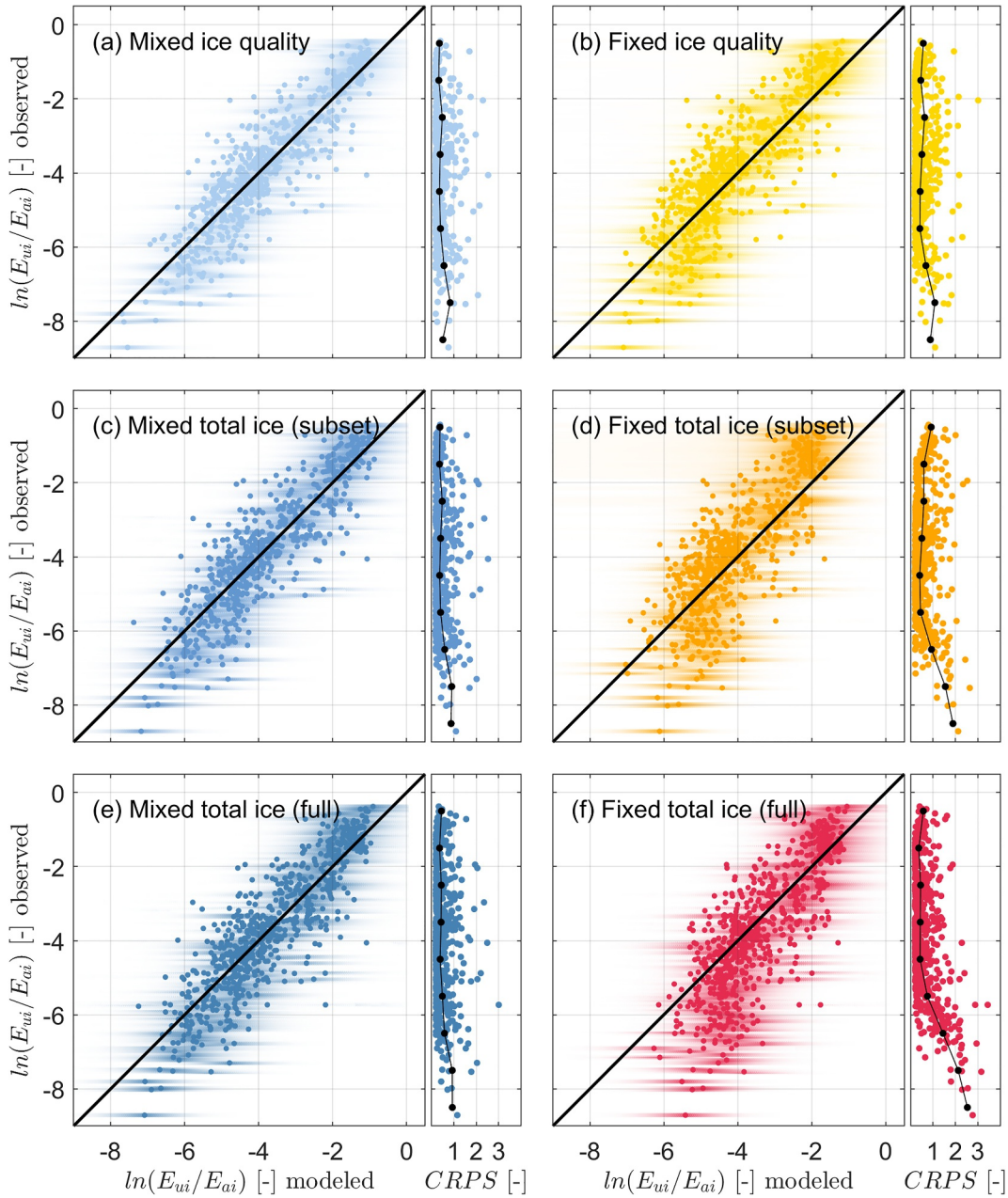

Figure 3. Comparison between observed and modeled values of $\ln(E_{ui}/E_{ai})$. Points represent median predictions, and shaded areas indicate the full distributions. Panels (a, c, and e) show results from the mixed model, panels (b, d, and f) show results using only the fixed component. Each row corresponds to a different modeling setup: (a–b) ice quality data, (c–d) total ice data for the same subset of lakes, and (e–f) total ice data from the full data set. Side panels display Continuous Ranked Probability Score distributions, with black lines indicating the median within bins of $\Delta \ln(E_{ui}/E_{ai}) = 1$.

these expected changes in ice and snow, our optical parameter estimates provide a robust basis for forecasting under-ice irradiance regimes under ongoing and future climate change, as further elaborated in the outlook below. At the same time, uncertainty in snow and white ice optical properties and thickness highlights the need for sustained, season-long monitoring and improved characterization of white ice structure across a broader range of lakes to refine future projections.

4. Conclusions and Outlook

A Bayesian modeling framework was developed to estimate the posterior probability distributions of diffuse attenuation coefficients and albedos for black ice, white ice, total ice, and snow in lakes using a large data set. By incorporating data from diverse lake environments, the model provides robust and generalizable estimates of these optical properties of ice and snow, with full posterior distributions that offer more than single-value estimates and enable improved quantification of uncertainty. The results demonstrate that the model performs well when ice quality data is available and provides reasonable estimates when only total ice thickness is used. However, future studies must explicitly examine the role of cDOM, within and beneath lake ice, as well as how freeze-thaw events redistribute cDOM and alter ice optical properties, since these processes can strongly regulate light penetration (Lei et al., 2011), yet remain an unknown factor (Arsenault et al., 2026). Compared to literature values that are often sparse, isolated, and case-specific, our approach reduces data variability, leading to transferable estimates that can be applied when in situ measurements are not available.

The outcomes of this study align with several key areas of environmental research and modeling captured in 100 pressing questions on ice that need to be addressed (Culpepper et al., 2025). These include (a) large-scale modeling of land-atmosphere interactions in the Northern Hemisphere, (b) assessing lake responses to climate change, (c) advancing research in under-ice physics and ecology, and (d) interpreting remote sensing data on lake-ice coverage and surface radiation balance. In the absence of high-resolution in situ monitoring of lake-ice properties, the outcomes of our Bayesian modeling can be readily integrated into both deterministic (e.g., Flake, GLM, MyLake, Simstrat (Moore et al., 2021)) and probabilistic (e.g., Williams et al. (2004); Abdelhady and Troy (2025)) lake-ice models, supporting lake-atmosphere coupling through improved albedo parameterizations in both real-time numerical weather prediction and global climate models, including studies that rely on idealized lake representations (Dibike et al., 2012). Models that explicitly resolve ice stratigraphy (e.g., GLM, MyLake, Simstrat) further benefit from the layer-specific optical parameters derived in this study, enabling improved predictions of under-ice irradiance that are critical for studies of under-ice physics and ecology. With the ongoing advancement of satellite observations, lake-ice properties such as total thickness and albedo can now be routinely monitored (e.g., Li et al. (2022); Mangilli et al. (2022)). When integrated with remote sensing algorithms, our results have the potential to improve the accuracy of these estimates, offering more reliable data for global climate models and improving predictions of both ecological and atmospheric processes. Ultimately, our findings contribute to a more comprehensive understanding of lake-ice dynamics, with broader implications for climate, lake ecosystems, and the use and management of lakes.

Conflict of Interest

The authors declare no conflicts of interest relevant to this study.

Availability Statement

Ice thickness, irradiance data, and metadata, along with the results of the Bayesian modeling and the *R* scripts used, are made publicly available at (Donini et al., 2025). Specifically, the results of the Bayesian modeling include probabilistic distributions of the albedos and diffuse attenuation coefficients for irradiance for the different ice and snow layers. The authors declare there are no conflicts of interest for this manuscript.

Acknowledgments

This project was initiated by an United States National Science Foundation (US NSF) funded workshop on Integrating limnological, remote sensing, and modeling approaches to understand global lake-ice dynamics (2033672). SP and GD acknowledge the Italian Ministry of Universities and Research (MUR), in the framework of the project DICAM-EXC (Departments of Excellence 2023–2027, Grant L232/2016). GAW, EJ and KV received financial support from the Swedish Research Council (VR-Grant. 2020-03222 and 2025-04711), the Royal Swedish Academy of Agriculture and Forestry (KSLA) and FORMAS-Grant. 2020–01091. HAD and Wisconsin data collection was supported by US NSF under Cooperative Agreement #DEB-2025982. RLN and Lake Simcoe data collection was supported by Environment Canada's Lake Simcoe Clean-up Fund (LSCUF; REHS, PJD) and NSERC (HMB, PJD, SLS, JJH: RGPIN-250060-20). Saskatchewan data was supported by CUPE PDF to RLN, Global Institute for Water Security at the University of Saskatchewan (GIWS; HMB, JJH), and the Saskatchewan Water Security Agency (JJH: WSA-2012A-0001). JR and Lakes Lacawac and Waynewood data collection was supported by the US NSF (award number 2434390). IAA studies were carried out under the state assignment of the Limnological Institute of SB RAS (FWSR-2026-0009). GZ, NP, RZ, IN studies and data collection were carried out under the state assignment of the NWPI of KarRC of RAS (FMEN-2026-0011). Thank you to Andrey Mitrokhov for field work assistance. IF studies were supported by the Institute of Botany after A.L. Takhtajyan National Academy of Sciences of the Republic of Armenia. MAX acknowledges support from Canada's Natural Sciences and Engineering Council and Canada Research Chair for data collection in the Kawartha Highland Lakes. Thank you to Claire Stevens for field work assistance. Open access publishing facilitated by Universita degli Studi di Trento, as part of the Wiley - CRUI-CARE agreement.

References

Abdelhady, H. U., & Troy, C. D. (2025). A deep learning approach for modeling and hindcasting lake michigan ice cover. *Journal of Hydrology*, *649*, 132445. https://doi.org/10.1016/j.jhydrol.2024.132445

Ariano, S. S., & Brown, L. C. (2019). Ice processes on medium-sized north-temperate lakes. *Hydrological Processes*, *33*(18), 2434–2448. https://doi.org/10.1002/hyp.13481

Arsenault, A. J., Pearce, N. J. T., Ozersky, T., D'Amario, S. C., Shchapov, K., Carrick, H. J., et al. (2026). Dissolved organic matter composition in the laurentian great lakes ice and its contribution to spring melt. *Journal of Geophysical Research: Biogeosciences*, *131*(2), e2025JG009367. https://doi.org/10.1029/2025JG009367

Arst, H., Erm, A., Leppäranta, M., & Reinart, A. (2006). Radiative characteristics of ice-covered fresh-and brackish-water bodies. *Proceedings of the Estonian Academy of Sciences: Geology*, *55*(1), 3–23. https://doi.org/10.3176/geol.2006.1.01

Ashton, G. D. (2011). River and lake ice thickening, thinning, and snow ice formation. *Cold Regions Science and Technology*, *68*(1–2), 3–19. https://doi.org/10.1016/j.coldregions.2011.05.004

Aslamov, I., Kirillin, G., Makarov, M., Kucher, K., Gnatovsky, R., & Granin, N. (2021). Autonomous system for lake ice monitoring. *Sensors*, *21*(24), 8505. https://doi.org/10.3390/s21248505

Barrett, D. C., & Wrona, F. J. (2025). Evaluating the influence of snow and ice conditions on under-ice light regimes, dissolved oxygen, and primary production in shallow lakes using controlled manipulative systems. *Limnology & Oceanography*, *70*(3), 599–616. https://doi.org/10.1002/lno.12788

Block, B. D., Denfeld, B. A., Stockwell, J. D., Flaim, G., Grossart, H.-P. F., Knoll, L. B., et al. (2019). The unique methodological challenges of winter limnology. *Limnology and Oceanography: Methods*, *17*(1), 42–57. https://doi.org/10.1002/lom3.10295

Bolsenga, S. J. (1969). Total albedo of great lakes ice. *Water Resources Research*, *5*, 1132–1133. https://doi.org/10.1029/WR005i005p01132

Bolsenga, S. J. (1977). Short note: Preliminary observations on the daily variation of ice albedo. *Journal of Glaciology*, *18*(80), 517–521. https://doi.org/10.3189/S0022143000021171

Bolsenga, S. J. (1981). Radiation transmittance through lake ice in the 400–700 nm range. *Journal of Glaciology*, *27*(95), 57–66. https://doi.org/10.3189/S0022143000011229

Bouffard, D., & Wüest, A. (2019). Annual review of fluid mechanics convection in lakes. *Annual Review of Fluid Mechanics*, *51*(1), 189–215. https://doi.org/10.1146/annurev-fluid-010518-040506

Bouffard, D., Zdorovennova, G., Bogdanov, S., Efremova, T., Lavanchy, S., Palshin, N., et al. (2019). Under-ice convection dynamics in a boreal lake. *Inland Waters*, *9*(2), 142–161. https://doi.org/10.1080/20442041.2018.1533356

Bramburger, A. J., Ozersky, T., Silsbe, G. M., Crawford, C. J., Olmanson, L. G., & Shchapov, K. (2023). The not-so-dead of winter: Underwater light climate and primary productivity under snow and ice cover in inland lakes. *Inland Waters*, *13*, 1–12. https://doi.org/10.1080/20442041.2022.2102870

Cao, X., Lu, P., Leppäranta, M., Arvola, L., Huotari, J., Shi, X., et al. (2021). Solar radiation transfer for an ice-covered lake in the central asian arid climate zone. *Inland Waters*, *11*(1), 89–103. https://doi.org/10.1080/20442041.2020.1790274

Cheng, Y., Cheng, B., Zheng, F., Vihma, T., Kontu, A., Yang, Q., & Liao, Z. (2020). Air/snow, snow/ice and ice/water interfaces detection from high-resolution vertical temperature profiles measured by ice mass-balance buoys on an Arctic lake. *Annals of Glaciology*, *61*(83), 309–319. https://doi.org/10.1017/aog.2020.51

Culpepper, J., Jakobsson, E., Weyhenmeyer, G. A., Hampton, S. E., Obertegger, U., Shchapov, K., et al. (2024). Lake ice quality in a warming world. *Nature Reviews Earth & Environment*, *5*(10), 671–685. https://doi.org/10.1038/s43017-024-00590-6

Culpepper, J., Sharma, S., Gunn, G., Magee, M. R., Meyer, M. F., Anderson, E. J., et al. (2025). One-hundred fundamental, open questions to integrate methodological approaches in lake ice research. *Water Resources Research*, *61*(5), e2024WR039042. https://doi.org/10.1029/2024WR039042

Dibike, Y., Prowse, T., Bonsal, B., Rham, L. d., & Saloranta, T. (2012). Simulation of north american lake-ice cover characteristics under contemporary and future climate conditions. *International Journal of Climatology*, *32*(5), 695–709. https://doi.org/10.1002/joc.2300

Donini, G., Piccolroaz, S., & Agostinelli, C. (2025). Supporting material for "Bayesian estimates of ice optical properties for lake ice modeling" [dataset]. *Zenodo*. https://doi.org/10.5281/zenodo.15689651

Dugan, H. A., Obryk, M. K., Gooseff, M. N., Doran, P. T., Chiuchiolo, A. L., Lawrence, J. P., & Priscu, J. C. (2025). Ice thickness regulates heat flux in permanently ice-covered lakes. *Limnology & Oceanography*, *70*(9), 2556–2568. https://doi.org/10.1002/lno.70151

Fritsen, C. H., & Priscu, J. C. (1999). Seasonal change in the optical properties of the permanent ice cover on lake bonney, Antarctica: Consequences for lake productivity and phytoplankton dynamics. *Limnology & Oceanography*, *44*(2), 447–454. https://doi.org/10.4319/lo.1999.44.2.0447

Garcia, S. L., Szekely, A. J., Bergvall, C., Schattenhofer, M., & Peura, S. (2019). Decreased snow cover stimulates under-ice primary producers but impairs methanotrophic capacity. *mSphere*, *4*(1), e00626-18. https://doi.org/10.1128/msphere.00626-18

Gneiting, T., & Raftery, A. E. (2007). Strictly proper scoring rules, prediction, and estimation. *Journal of the American Statistical Association*, *102*(477), 359–378. https://doi.org/10.1198/016214506000001437

Grenfell, T. C., & Perovich, D. K. (2004). Seasonal and spatial evolution of albedo in a snow-ice-land-ocean environment. *Journal of Geophysical Research*, *109*(C1). https://doi.org/10.1029/2003jc001866

Hampton, S. E., Galloway, A. W. E., Powers, S. M., Ozersky, T., Woo, K. H., Batt, R. D., et al. (2017). Ecology under lake ice. *Ecology Letters*, *20*(1), 98–111. https://doi.org/10.1111/ele.12699

Hampton, S. E., Moore, M. V., Ozersky, T., Stanley, E. H., Polashenski, C. M., & Galloway, A. W. (2015). Heating up a cold subject: Prospects for under-ice plankton research in lakes. *Journal of Plankton Research*, *37*(2), 277–284. https://doi.org/10.1093/plankt/fbv002

Hampton, S. E., Powers, S. M., Dugan, H. A., Knoll, L. B., McMeans, B. C., Meyer, M. F., et al. (2024). Environmental and societal consequences of winter ice loss from lakes. *Science*, *386*(6718), eadl3211. https://doi.org/10.1126/science.adl3211

Heron, R., & Woo, M.-K. (1994). Decay of a High Arctic lake-ice cover: Observations and modelling. *Journal of Glaciology*, *40*(135), 283–292. https://doi.org/10.3189/s0022143000007371

Hoffman, M. D., & Gelman, A. (2014). The no-u-turn sampler: Adaptively setting path lengths in hamiltonian monte carlo. *Journal of Machine Learning Research*, *15*(1), 1593–1623.

Huang, L., Timmermann, A., Lee, S.-S., Rodgers, K. B., Yamaguchi, R., & Chung, E.-S. (2022). Emerging unprecedented lake ice loss in climate change projections. *Nature Communications*, *13*(1), 5798. https://doi.org/10.1038/s41467-022-33495-3

Jakkila, J., Leppäranta, M., Kawamura, T., Shirasawa, K., & Salonen, K. (2009). Radiation transfer and heat budget during the ice season in Lake Pääjärvi, Finland. *Aquatic Ecology*, *43*(3), 681–692. https://doi.org/10.1007/s10452-009-9275-2

Jiang, J., & Nguyen, T. (2021). *Linear and generalized linear mixed models and their applications*. Springer.

Kirillin, G. B., Leppäranta, M., Terzhevik, A., Granin, N., Bernhardt, J., Engelhardt, C., et al. (2012). Physics of seasonally ice-covered lakes: A review. *Aquatic Sciences*, *74*(4), 659–682. https://doi.org/10.1007/s00027-012-0279-y

Kirillin, G. B., Shatwell, T., & Wen, L. (2021). Ice-covered lakes of Tibetan Plateau as solar heat collectors. *Geophysical Research Letters*, *48*(14), e2021GL093429. https://doi.org/10.1029/2021GL093429

Lang, J., Lyu, S., Li, Z., Ma, Y., & Su, D. (2018). An investigation of ice surface albedo and its influence on the high-altitude lakes of the Tibetan Plateau. *Remote Sensing*, *10*(2), 218. https://doi.org/10.3390/rs10020218

Langbehn, T. J., & Varpe, O. (2017). Sea-ice loss boosts visual search: Fish foraging and changing pelagic interactions in polar oceans. *Global Change Biology*, *23*(12), 5318–5330. https://doi.org/10.1111/gcb.13797

Lei, R., Leppäranta, M., Erm, A., Jaatinen, E., & Pärn, O. (2011). Field investigations of apparent optical properties of ice cover in Finnish and Estonian lakes in winter 2009. *Estonian Journal of Earth Sciences*, *60*(1), 50–64. https://doi.org/10.3176/earth.2011.1.05

Leppäranta, M. (2023). *Freezing of lakes and the evolution of their ice cover* (2nd ed. ed.). Springer. https://doi.org/10.1007/978-3-031-25605-9

Leppäranta, M., Lindgren, E., Wen, L., & Kirillin, G. (2019). Ice cover decay and heat balance in Lake Kilpisjärvi in arctic tundra. *Journal of Limnology*, *78*(2), 163–175. https://doi.org/10.4081/jlimnol.2019.1879

Leppäranta, M., Terzhevik, A., & Shirasawa, K. (2010). Solar radiation and ice melting in Lake Vendyurskoe, Russian Karelia. *Hydrology Research*, *41*(1), 60–62. https://doi.org/10.2166/nh.2010.122

Li, X., Long, D., Huang, Q., & Zhao, F. (2022). The state and fate of lake ice thickness in the northern hemisphere. *Science Bulletin*, *67*(5), 537–546. https://doi.org/10.1016/j.scib.2021.10.015

Li, Z., Ao, Y., Lyu, S., Lang, J., Wen, L., Stepanenko, V., et al. (2018). Investigation of the ice surface albedo in the Tibetan Plateau lakes based on the field observation and MODIS products. *Journal of Glaciology*, *64*(245), 506–516. https://doi.org/10.1017/jog.2018.35

Mangilli, A., Thibaut, P., Duguay, C. R., & Murfitt, J. (2022). A new approach for the estimation of lake ice thickness from conventional radar altimetry. *IEEE Transactions on Geoscience and Remote Sensing*, *60*, 1–15. https://doi.org/10.1109/TGRS.2022.3186253

McCrystall, M. R., Stroeve, J., Serreze, M., Forbes, B. C., & Screen, J. A. (2021). New climate models reveal faster and larger increases in arctic precipitation than previously projected. *Nature Communications*, *12*(1), 6765. https://doi.org/10.1038/s41467-021-27031-y

Michel, B., & Ramseier, R. O. (1971). Classification of river and lake ice. *Canadian Geotechnical Journal*, *8*(1), 36–45. https://doi.org/10.1139/t71-004

Mobley, C. (2001). Radiative transfer in the ocean. In J. K. Cochran, H. J. Bokuniewicz, & P. L. Yager (Eds.), *Encyclopedia of ocean sciences* (3rd ed.) (3rd ed. p. 379–388). : Academic Press. https://doi.org/10.1016/B978-0-12-409548-9.04311-6

Moore, T. N., Mesman, J. P., Ladwig, R., Feldbauer, J., Olsson, F., Pilla, R. M., et al. (2021). Lakeensemblr: An r package that facilitates ensemble modelling of lakes. *Environmental Modelling & Software*, *143*, 105101. https://doi.org/10.1016/j.envsoft.2021.105101

Mullen, P., & Warren, S. (1988). Theory of the optical properties of lake ice. *Journal of Geophysical Research*, *93*(D7), 8283–8458. https://doi.org/10.1029/JD093iD07p08403

Niu, R., Wen, L., Wang, C., Tang, H., & Leppäranta, M. (2025). Air–ice–water temperature and radiation transfer via different surface coverings in ice-covered qinghai lake of the Tibetan Plateau. *Water*, *17*(2), 142. https://doi.org/10.3390/w17020142

Obertegger, U., Obrador, B., & Flaim, G. (2017). Dissolved oxygen dynamics under ice: Three winters of high-frequency data from Lake Tovel. *Italy. Water Resources Research*, *53*(8), 7234–7246. https://doi.org/10.1002/2017WR020599

Palshin, N. I., Zdorovennova, G. E., Zdorovennov, R. E., Efremova, T. V., Gavrilenko, G. G., & Terzhevik, A. Y. (2019). Effect of under-ice light intensity and convective mixing on chlorophyll a distribution in a small mesotrophic lake. *Water Resources*, *46*(3), 384–394. https://doi.org/10.1134/S0097807819030175

Pernica, P., North, R. L., & Baulch, H. M. (2017). In the cold light of day: The potential importance of under-ice convective mixed layers to primary producers. *Inland Waters*, *7*(2), 138–150. https://doi.org/10.1080/20442041.2017.1296627

Perovich, D. K. (2007). Light reflection and transmission by a temperate snow cover. *Journal of Glaciology*, *53*(181), 201–210. https://doi.org/10.3189/172756507782202919

Petrov, M. P., Terzhevik, A. Y., Palshin, N. I., Zdorovennov, R. E., & Zdorovennova, G. E. (2005). Absorption of solar radiation by snow-and-ice cover of lakes. *Water Resources*, *32*(5), 546–554. https://doi.org/10.1007/s11268-005-0063-7

Pongracz, A., Wårlind, D., Miller, P. A., Gustafson, A., Rabin, S. S., & Parmentier, F.-J. W. (2024). Warming-induced contrasts in snow depth drive the future trajectory of soil carbon loss across the arctic-boreal region. *Communications Earth & Environment*, *5*(1), 684. https://doi.org/10.1038/s43247-024-01838-1

Quante, L., Willner, S. N., Middelanis, R., & Levermann, A. (2021). Regions of intensification of extreme snowfall under future warming. *Scientific Reports*, *11*(1), 16621. https://doi.org/10.1038/s41598-021-95979-4

Sherstyankin, P. P. (1975). Experimental studies of the under-ice light field of Lake Baikal. *USSR Academy of Sciences*. Nauka

Socha, E., Gorsky, A., Lottig, N. R., Gerrish, G., Whitaker, E. C., & Dugan, H. A. (2023). Under-ice plankton community response to snow removal experiment in bog lake. *Limnology & Oceanography*, *68*(5), 1001–1018. https://doi.org/10.1002/lno.12319

Solarski, M., & Retała, M. (2020). Ice regime of the kozłowa góra reservoir (southern Poland) as an indicator of changes of the thermal conditions of ambient air. *Water*, *12*(9). https://doi.org/10.3390/w12092435

Song, S., Li, C., Shi, X., Zhao, S., Tian, W., Li, Z., et al. (2019). Under-ice metabolism in a shallow lake in a cold and arid climate. *Freshwater Biology*, *64*(10), 1710–1720. https://doi.org/10.1111/fwb.13363

Stan Development Team. (2024). Stan reference manual (Vol. *v2.36.0*). Retrieved from https://mc-stan.org

Suarez, E. L., Tiffay, M.-C., Kalinkina, N., Tchekryzheva, T., Sharov, A., Tekanova, E., et al. (2019). Diurnal variation in the convection-driven vertical distribution of phytoplankton under ice and after ice-off in large Lake Onego (Russia). *Inland Waters*, *9*(2), 193–204. https://doi.org/10.1080/20442041.2018.1559582

Vehmaa, A., & Salonen, K. (2009). Development of phytoplankton in Lake Pääjärvi (Finland) during under-ice convective mixing period. *Aquatic Ecology*, *43*(3), 693–705. https://doi.org/10.1007/s10452-009-9273-4

Warren, S. G. (1982). Optical properties of snow. *Reviews of Geophysics*, *20*(1), 67–89. https://doi.org/10.1029/rg020i001p00067

Weyhenmeyer, G. A., Obertegger, U., Rudebeck, H., Jakobsson, E., Jansen, J., Zdorovennova, G., et al. (2022). Towards critical white ice conditions in lakes under global warming. *Nature Communications*, *13*(1), 4974. https://doi.org/10.1038/s41467-022-32633-1

Williams, G., Layman, K. L., & Stefan, H. G. (2004). Dependence of lake ice covers on climatic, geographic and bathymetric variables. *Cold Regions Science and Technology*, *40*(3), 145–164. https://doi.org/10.1016/j.coldregions.2004.06.010

Wu, L. (2009). *Mixed effects models for complex data*. CRC Press.

Yang, B., Wells, M. G., Li, J., & Young, J. (2020). Mixing, stratification, and plankton under lake-ice during winter in a large lake: Implications for spring dissolved oxygen levels. *Limnology & Oceanography*, *65*(11), 2713–2729. https://doi.org/10.1002/lno.11543

Zdorovennova, G., Palshin, N., Efremova, T., Zdorovennov, R., Gavrilenko, G., Volkov, S., et al. (2018). Albedo of a small ice-covered boreal lake: Daily, meso-scale and interannual variability on the background of regional climate. *Geosciences*, *8*(6), 206. https://doi.org/10.3390/geosciences8060206

Zdorovennova, G., Zdorovennov, R., Palshin, N., & Terzhevik, A. (2013). Optical properties of the ice cover on Vendyurskoe Lake, Russian Karelia (1995-2012). *Annals of Glaciology*, *54*(62), 121–124. https://doi.org/10.3189/2013AoG62A179

Zhao, W., Huang, W., Li, R., Zhang, J., Zhang, C., Li, Z., & Lin, Z. (2024). Solar radiation transfer in an ice-covered lake at different snow thicknesses. *Hydrological Sciences Journal*, *69*(2), 195–206. https://doi.org/10.1080/02626667.2023.2297075